*Traffic 2002; **3**: 000–000*
Blackwell Munksgaard

ISSN 1398-9219

Regulation of Peptidergic Vesicle Mobility by Secretagogues

C. L. Washburn[1], J. E. Bean[1], M. A. Silverman[1], M. J. Pellegrino[2], P. A. Yates[1] and R. G. Allen[1], *

[1]Center for Research on Occupational and Environmental Toxicology (CROET), The Vollum Institute and [2]The Neuroscience Graduate Program, Oregon Health and Science University, 3181 Sam Jackson Park Road, Portland, OR 97201, USA
**Corresponding author: R. G. Allen,allenr@ohsu.edu*

Neuropeptides are released into the extracellular space from large secretory granules. In order to reach their release sites, these granules are translocated on microtubules and thought to interact with filamentous actin as they approach the cell membrane. We have used a green fluorescent protein-tagged neuropeptide prohormone (prepro-orphanin FQ) to visualize vesicle trafficking dynamics in NS20Y cells and cultures of primary hippocampal neurons. We found that the majority of secretory granules were mobile and accumulated at both the tips of neurites as well as other apparently specialized cellular sites. We also used live-cell imaging to test the notion that peptidergic vesicle mobility was regulated by secretagogues. We show that treatment with forskolin appeared to increase vesicle rates of speed, while depolarization with high K^+ had no effect, even though both treatments stimulated neuropeptide secretion. In cultured hippocampal neurons the green fluorescent protein-tagged secretory vesicles were routed to both dendrites and axons, indicating that peptidergic vesicle transport was not polarized. Basal peptidergic vesicle mobility rates in hippocampal neurons were the same as those in NS20Y cells. Taken together, these studies suggest that secretory vesicle mobility is regulated by specific classes of secretagogues and that neuropeptide containing secretory vesicles may be released from dendritic structures.

Key words:

Received 4 April 2002,revised andaccepted for publication 23 July 2002

Neuropeptide secretion is a process that is distinct from classical transmitter release. It is a process that takes place on the order of seconds to minutes and is not associated with synaptic active zones (1). Neuropeptide containing secretory granules (large dense-core vesicles; LDCVs) are not refilled locally and thus have to be synthesized in the cell body and shipped to release sites via interactions with microtubules(2–4). Following the translocation of vesicles on microtubules to their release sites, the regulation of docking and fusion of vesicles must occur to complete the neurosecretory process. At this step in neurosecretion, it is thought that LDCVs interact with filamentous (F)-actin at specialized release sites(5–7). At the present time, it is not understood how the increased demand for newly made and existing peptidergic vesicles is met during periods of stimulated secretion.

Molecular motors, such as the dynein and kinesin family of molecules, transport vesicular cargo and have been the subject of intense interest in recent years (8,9). For instance, dynein and kinesinII interact with microtubules to regulate bidirectional organelle transport (10). Further, hyperphosphorylation of kinesin light chain inhibits kinesin-mediated transport of mitochondria (11). Also, the protein kinase A pathway inhibits anterograde axonal transport of vesicles (12). Kinesin motors transport organelles in an ATP- and microtubule-dependent fashion and, along with their associated GTPases, scaffolds and adaptor proteins, may be potential sites of regulating vesicle mobility, thus altering delivery rates of vesicular cargo (8).

Previous studies used a green fluorescent protein (GFP)-tagged peptide precursor (preproatrial natriuretic factor) combined with optical measurement of stimulated secretion and determined that neuronal peptide release is limited by secretory granule mobility (13). Additional observations from studies using PC12 cells have led to the hypothesis that the mobile, rather than stationary pool of peptidergic vesicles is more efficiently recruited for release (13). In these studies there was no definition of mobility, and they raise the question whether peptidergic vesicle mobility is regulated.

Here, we test the hypothesis that peptidergic vesicle translocation rates are regulated by secretagogues. To accomplish this we have developed a model system to visualize peptidergic vesicle dynamics, using neuronally derived NS20Y cells stably transfected with a cDNA vector encoding the orphanin FQ (OFQ/nociceptin) prohormone (ppOFQ) fused to GFP (eGFP). This fusion protein was routed into LDCVs, and their dynamics in response to secretagogues could be followed in single cells using time-lapse imaging. Even though both high K^+ and forskolin stimulate OFQ peptide secretion, we found that forskolin stimulation of NS20Y cells resulted in the increase of vesicle translocation rates, while depolarization with high K^+ did not, thus suggesting that only certain classes of secretagogues can regulate vesicle mobility. In addition, we report the novel finding that peptidergic vesicles

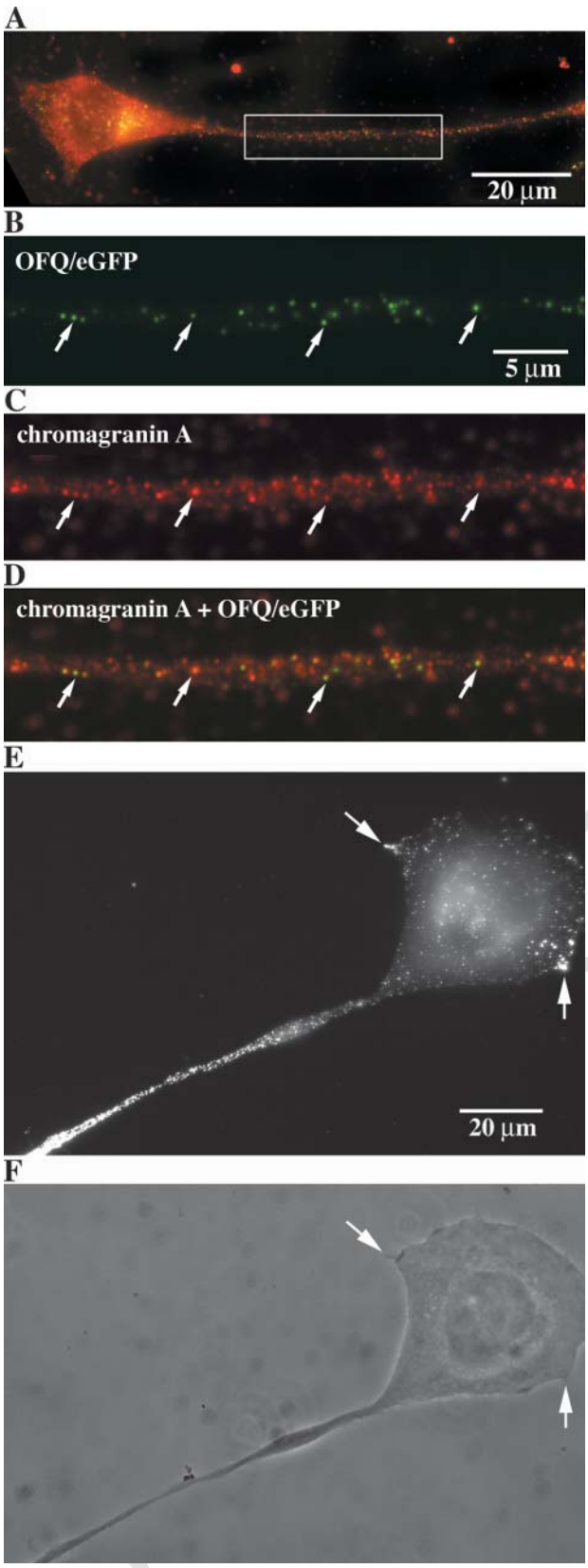

Figure 1: Co-localization of OFQ/eGFP-tagged vesicles and chromogranin A (chrA) in NS20Y OFQ/eGFP (SC1) cells. (A)An NS20Y (SC1) cell expressing OFQ/eGFP and stained for ChrA at low magnification. Bar = 20 μm. The rectangle shown is used for 2B–D.(B)OFQ/eGFP-tagged structures are punctate green fluorescence.(C)Immuno-fluorescence using rhodamine conjugate second antibody to the ChrA antiserum.(D)Red and green fluorescence overlay. The arrows show the particles that line up in the overlay. In particular, notice the three vesicles in a row starting at the far left.(E)Fluorescence microscopy of an NS20Y cell with a long process showing accumulation of vesicles at the tip. The arrows show two 'protoprocess' accumulating peptidergic vesicles.(F)Bright-field of the cell shown in A. Q25

traffic to both the dendrites and axons of cultured hippocampal neurons, suggesting that neuropeptides also may be released from dendritic structures.

Results

Expression of ppOFQ/eGFP in NS20Y cells

Figure 1(A) shows an NS20Y cell stably expressing OFQ/eGFP and immunostained for chromogranin A (ChrA), a marker of peptidergic granules. We found a punctate pattern of fluorescence in NS20Y cells stably expressing OFQ/eGFP, suggesting that the OFQ/eGFP fusion protein was routed into LDCV-'like' structures (Figure 1B).Figure 1(C) shows that ChrA immunofluorescence is punctate in NS20Y (SC1) cells and that every OFQ/eGFP-tagged structure colocalizes with ChrA (Figure 1D). The representative arrows point out examples of colocalization. We also found that approximately 40% of the ChrA staining vesicles colocalized with OFQ/eGFP fluorescence in the field shown here, suggesting that peptidergic vesicles are a major subpopulation of ChrA-containing vesicles.Figure 1(E) shows another representative NS20Y cell. Not only did peptidergic vesicles accumulate in long processes, but there were slight bulges with accumulations of vesicles (see figure legend for details) we called 'protoprocesses'. Figure 1(F) is a bright-field photomicrograph of the cell shown in Figure 1(E). These observations indicate that the peptidergic vesicle distribution in the NS20Y cells was not random, as vesicles accumulated at specific sites in the cell body and tips of neurites. In addition, these data show that ChrA and peptidergic vesicles were not excluded from any processes, and thus do not appear to be polarized in the NS20Y cells.

Observations of peptidergic vesicle mobility

In our initial observations of OFQ-tagged peptidergic vesicles, we found that the particles were universally spheres less than 350 nm in diameter, suggesting that the ppOFQ/GFP fusion protein was routed into LDCVs in the regulated pathway and not the tubular shapes associated with cargo vesicles in the

constitutive pathway (2,14). The movements of most vesicles were multidirectional in the cell body and mostly bi-directional in the neurites, possibly due to special constraints. When vesicles accumulated in the tips of processes their movement became very restricted. Almost all of the vesicles would exhibit 'dancing' movements and then embark on saltations of 1–4 μm, or more. Figure 2 shows a representative NS20Y cell body and the movement tracks of four peptidergic vesicles during 60 frames of time-lapse imaging. The track-pattern displacements shown are typical of cell body vesicle movement. The bottom panel in Figure 2 shows the average rate of speed vs. distance traveled of 14 individual control vesicles imaged from three different cells, for 60 frames (2.5 min). It can be seen that the majority of vesicles translocate at rates of 0.1–0.2 μm/s (see below). These data also may be significant in supporting the notion that the faster a vesicle travels, the farther it travels.

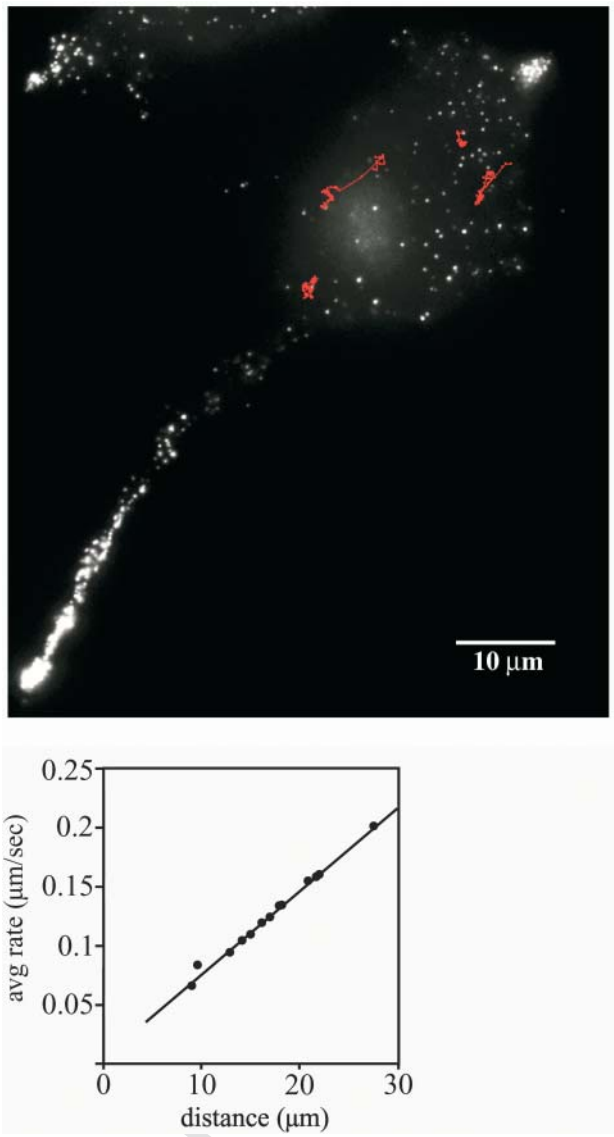

Figure 2: Peptidergic vesicle movement in NS20Y cells stably expressing ppOFQ/eGFP. In the top panel the red lines show the tracks of peptidergic vesicles in the cell body during a 2.5-min (60-frame) excursion. The bottom panel shows the average rate vs. distance of 15 individual vesicles. The solid lines are ± SEM of 60 frames for individual velocities. $R^2 = 0.996$ for best linear fit analysis.

Regulation of peptidergic vesicle mobility by secretagogues

Because these compounds stimulate neuropeptide secretion, we wanted to determine if either depolarization with high K^+ or treatment with forskolin altered vesicle translocation rates. During the first 30 frames (~ 1 min) no secretagogues were present, and during the second 30 frames either 10 μM forskolin or high K^+ media (60 mM) were perfused into the chamber. We also recorded time-lapse images for 60 frames in the absence of secretagogues (Figure 3A). The data gathered in the 60 frames were analyzed in several ways. First, the translocation rate (μm/s) in each frame was averaged for the initial 30 frames and the second 30 frames for each secretagogue. Figure 3(B) shows that 10 μM forskolin caused a significant increases in vesicle rate of speed, while depolarization with high K^+ did not (Figure 3C). In addition, we analyzed the data for changes in inward and outward vesicle movement, as well as changes in vesicle populations near to the membrane and in the cell body (inserts in panels 3A, B, and C). We found that secretagogues had no effects on either these parameters or vesicle populations.

Second, we plotted the velocity of a vesicle in each individual frame, for the entire 60 frames. Figure 4(A) shows that forskolin treatment caused a marked increase in the individual rates of translocation (note the increase in rate/frame, over the last 30 frames), while high K^+ did not (Figure 4B). Third, we averaged individual vesicle rates in each frame over the entire 60 frames. After the first 20–30 frames, median velocity increases sharply as a function of increasing time. Using a linear 'mixed effect' model (15), it was estimated that median translocation rate increases 32.8% every 30 s (95% confidence interval; 9.5–61.2% increase) in the forskolin-treated cells, but no significant slope difference was seen with high K^+ treatment (not shown). Further, vesicles show a rather large range of speed (0.1–0.5 μm/s) and can change velocity rapidly; even in 2.6 s. In addition, we have shown that both forskolin (16) and high K^+ (Figure 4B, insert) induce significant increases in OFQ peptide secretion from NS20Y cells. Q6

We also counted the number of stops a vesicle made during the control and secretagogue treatment periods. We found that there was no significant difference between the two and, in addition, the number of stops a vesicle made was only about 4–5 during the entire 60 frames. This indicates that the number of motor–microtubule associations did not appear to be altered by either forskolin or KCl. These results suggest that certain classes of regulators, even though they increase neuropeptide secretion, may or may not effect peptidergic vesicle movement and potential delivery rates to release sites. In addition, the increase in speed implies that forskolin in- Q7

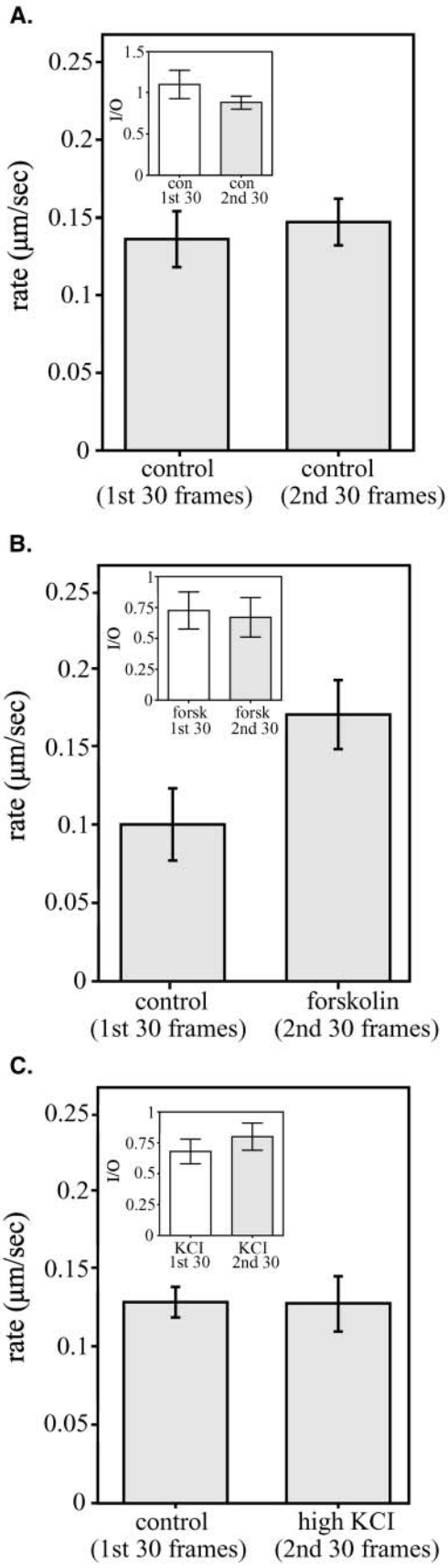

Figure 3: Regulation of peptidergic vesicle mobility by secretagogues. Cells were perfused with control solution; 3 cells (15 vesicles), 10 µM forskolin (3 cells, 6 vesicles) or 60 mM KCl (1 cell, 6 vesicles). Using the time-lapse images, individual vesicles were tracked for the entire 2.5 min (60 frames). Individual vesicle rates were averaged for control and treatment periods. $p = 0.002$ in paired t-test, using StatView® software, ± SEM. The inserts show the ratio of inward (I) vs. outward (O) vesicle movement during the first 30 frames and the last 30 frames. Error bars are ± SEM.

creased the granule run-length, thus inducing longer contact between the vesicle and the microtubule.

Expression of OFQ/eGFP in cultures of hippocampal neurons

We next wanted to examine the trafficking of peptidergic vesicles in living neurons. We transfected both the OFQ/eGFP and the OFQ/YFP vectors into 7–9-day-old cultures of hippocampal neurons, and examined the expression by fluorescence microscopy. Forty-eight hours after transfection, the OFQ/FP proteins had been synthesized, processed, packaged and shipped to the distal tips of the axons. In order to further substantiate the nonpolarized distribution of the peptidergic vesicles seen by visual inspection, we performed immunostaining for microtubule-associated protein 2 (MAP2), a marker for dendrites (17) and cotransfected OFQ/YFP and a CFP base vector to tag peptidergic vesicles and fill all processes with blue fluorescence. Figure 5 (arrows) shows yellow vesicles in dendritic structures stained for MAP2 (box A) as well as axonal structures fluorescing blue (box B). Boxes A and B are shown at higher magnification in the bottom panels of Figure 5. Figure 5(C) shows colocalization (left panel) of ChA (middle panel) and OFQ/eGFP (right panel) in LDCVs of hippocampal neurons. We found that 2–12% of ChrA staining colocalized with OFQ/YFP fluorescence in primary hippocampal neurons, a smaller vesicle subpopulation than in the NS20Y cells. Q8

In order to examine peptidergic vesicle mobility in living neurons we performed live-cell imaging. Figure 6 shows hippocampal neurons expressing OFQ/eGFP. Rectangles (A), (B) and (C) show three sets of consecutive frames capturing excursion events for distinct vesicles. Peptidergic vesicle trafficking rates in hippocampal neurons ranged from 0.04 to 0.5 µm/s, in good agreement with those vesicle velocities found in the NS20Y cells expressing OFQ/eGFP. We have also provided a movie of both NS20Y cells and hippocampal neurons that can be accessed at the site denoted in the Footnotes (Traffic.com). These data suggest that peptidergic vesicles are not polarized to axons and the shipment of peptidergic vesicles to dendrites raises the intriguing possibility of dendritic release of neuropeptides. Q9

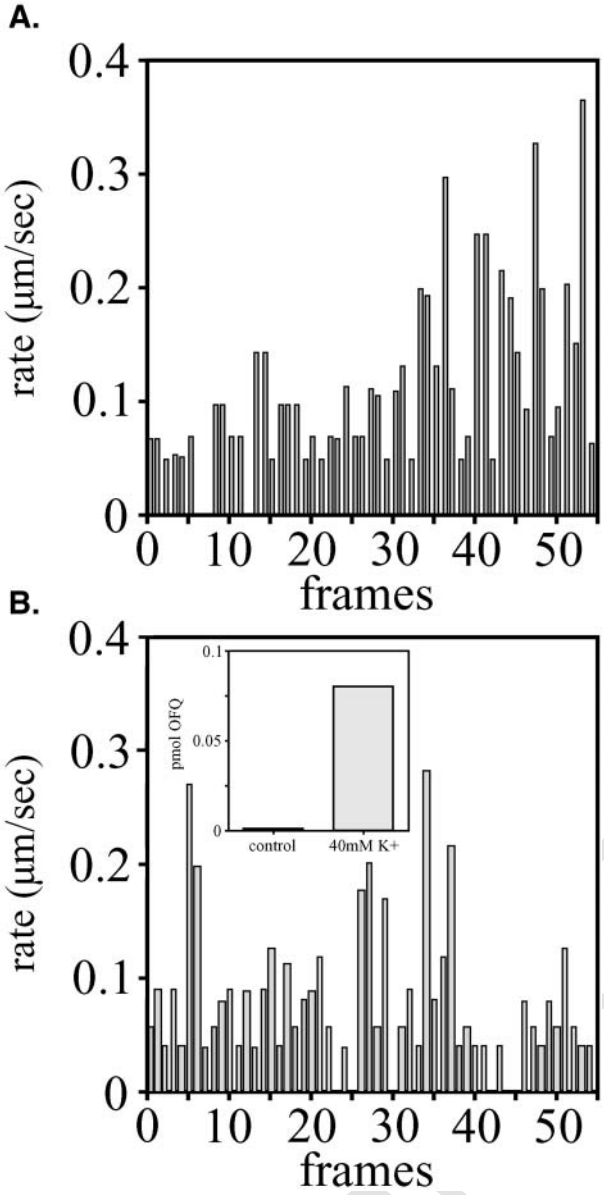

Figure 4: Regulation of individual vesicle velocities in NS20Y cells by frame in the presence of forskolin and high K^+. NS20Y cells were treated as inFigure 4. The graphs show the rates of vesicles in individual frames during the perfusion in the presence and absence of secretagogues. Note that rates increase in the second 30 frames of the forskolin treatment(A), while rates remain constant during the high KCl treatment(B).The insert shows duplicate T-flasks of NS20Y cells treated for 40 min with control or 40 mM KCl and the medium assayed OFQ peptide immunoreactivity.

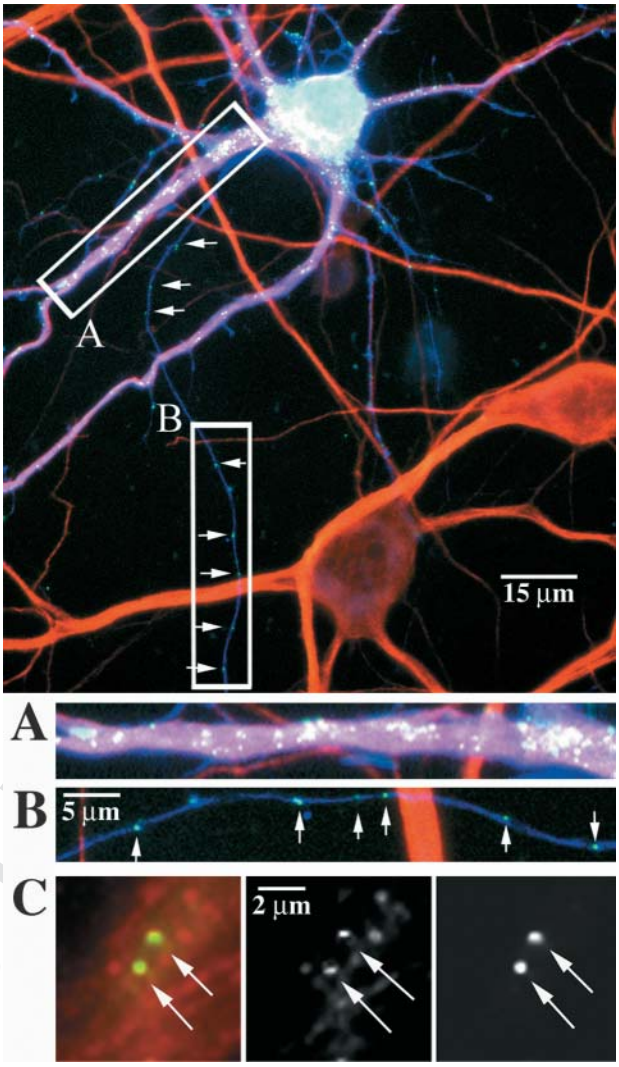

Figure 5: Peptidergic vesicles traffic to dendrites and axons in hippocampal neurons. Primary cultures of hippocampal neurons were cotransfected with the OFQ/yFP and cFP vectors and after 48 h the cells were fixed, permeabilized and immunostained for MAP2. The top panel shows a representative hippocampal neuron expressing YFP-tagged vesicles and immunostained for MAP2 (dendrites). The arrows indicate vesicles in axonal structures showing blue fluorescence. The rectangles A and B have been magnified in the lower panels. The bottom panels show hippocampal neurons expressing OFQ/GFP and immunostained for ChrA as described in the Results.

Discussion

Large dense-core vesicles (LDCVs): mobility and models of neuropeptide secretion

Neuropeptide secretion is controlled by elevations in intracellular calcium levels that can occur through a variety of effectors. This activity is different for the release of conventional neurotransmitters in that it is not associated with so-called 'active' zones. Since peptidergic vesicles must be synthesized in the cell body and transported to their release points, peptidergic secretion must be tightly controlled (1). The mechanisms that control kinetics and magnitude of secretory responses are not understood. In fact, it is not understand how the movement of any given class of neuronal organelle is regulated in response to changes in the extra-cellular environment (8).

Many of the studies addressing this problem have used PC12

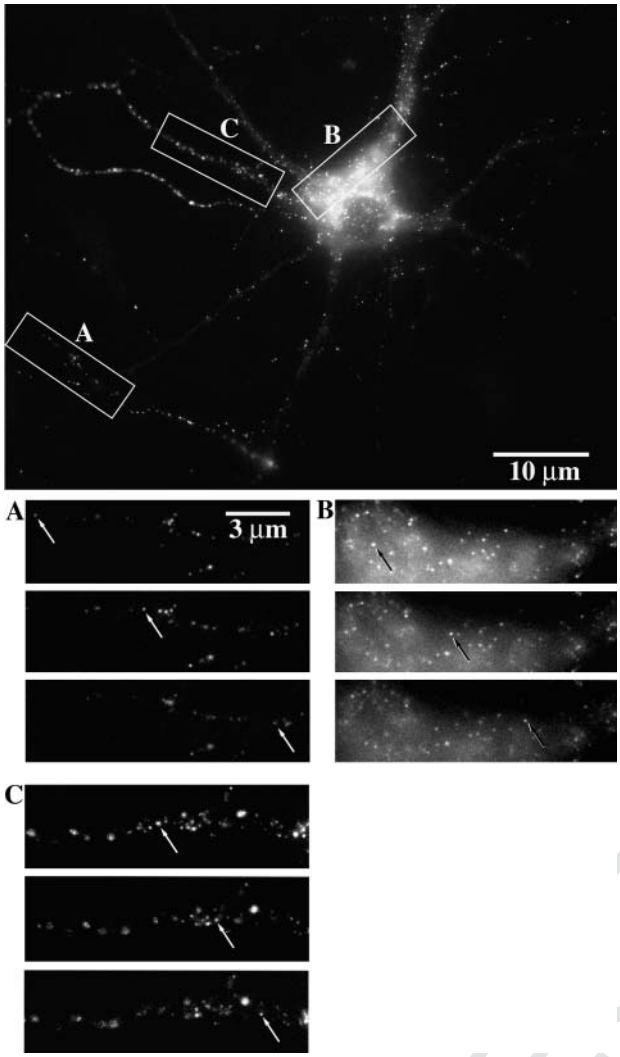

Figure 6: Peptidergic vesicle mobility in living hippocampal neurons. Hippocampal cultures were transfected as described in Materials and Methods, with the OFQ/eGFP vector and time-lapse imaging performed. The top panel shows a representative neuron expressing OFQ/eGFP. Rectangles A, B and C in the lower panels show three successive frames and the arrows indicate the movement of a single vesicle in a process (A), the cell body (B) and a dendrite (C). Individual vesicle rates of speed ranged between 0.04 and 0.5 μm/s.

Q10 cells and proteins or peptides fused to GFP. Burke et al. (13) used GFP-tagged preproatrial natriuretic factor to demonstrate that neuropeptides are slowly released from a limited pool of secretory granules. They also found that secretion does not specifically deplete a granule pool near the plasma membrane, which was one of the original tenets of the study. It was also concluded that sustained secretion might be limited by the number of mobile granules. These studies were extended and claim to show that rapidly moving vesicles were more efficiently recruited for release (18). More importantly, it was suggested that the mobile vesicles diffused randomly, suggesting that they were not tethered to the cytoskeleton. Our results show that a large proportion of the peptide-containing granules are mobile, and many of these motions do not appear to be random. Our studies agree with Han et al. (18) in that we never saw a disappear- Q11 ance of vesicles from the population congregating near the plasma membrane during short periods of stimulation. However, it may be that this pool is rapidly filled and there is never a depletion of vesicles.

Other studies have used GFP fusion proteins to study LDCV movement in the regulated secretory pathway (15,19) and in the constitutive pathway (2,14,20,21). Chao et al. (14), Wacker et al. (2) and Hirschberg et al. (20) found partical shapes of Q12 both tubules and spheres ranging from 1 to 1.8 μm in length, while Kaether et al. (15), Burke et al. (13) and Lochner et al. (19), found only spheres under 1 μm in diameter. It is interest- Q13 ing that the studies in the first group were investigating the constitutive pathway and the latter three studies were investigating the regulated pathway, because it appears that tubules and spheres are associated with the constitutive pathway and spheres are exclusively associated with the regulated pathway.

Hippocampal neurons have been shown to contain LDCVs associated with peptide processing (22). Our results revealed spheres less than 350 nm in diameter, indicating our OFQ/GFP fusion proteins were routed into LDCVs in both the NS20Y cells and cultured hippocampal neurons. Furthermore, OFQ/FP-tagged vesicles colocalized with ChrA staining in both hippocampal neurons and the NS20Y cells, suggesting again that the fusion protein was routed to LDCVs. We followed the areas of the 'protoprocesses' for several days (Allen, unpublished results), and found that the NS20Y cells formed protoprocesses that had accumulated vesicles, and then many of these processes grew into neurites. It is not known at the present time whether such an event takes place during normal neuronal development. In addition, pepticlergic vesicles trafficked to both dendrites and axons in hippocampal neurons, supporting recent findings that show Ca^{++} regulation of neuropeptide release from dendrites (23).

Processive motors, such as conventional kinesin, transport membrane organelles (3,4,8,9). However, transport of larger organelles may be accomplished by many motors working in concert or in a nonprocessive fashion. In studies with conventional kinesin, it has been shown that the motor takes several hundred steps per encounter with a microtubule. The run length can be increased by adding positive charges to the neck, coiled-coil region of the molecule and, conversely, negative charges decrease the run length (24). Other studies have shown that the phosphorylation of kinesin can increase its glide length (25). These two results do not correlate, since phosphorylation of kinesin would add a negative charge; however, the addition of charge might be at different sites. In addition, changes in phosphorylation may affect the association of kinesin (12,26–28) or dynein (29,30) with membranes. These data indicate that motor–organelle interactions can be controlled, but these studies were directed at under-

standing the regulation of directionality for vesicle movement and not the velocity of vesicle movement. A recent review by Duke suggests that teams of motors may come into play (31). It is clear that motor regulation is much more complicated than adding or removing charges.

At the present time, the molecular factors that govern run-length and velocity of motors and their cargo are poorly understood. Recently, Gelfand and coworkers addressed this problem using dispersal and aggregation of melanosomes as a model system (32). They found that during dispersion, myosin V functions as a 'ratchet', increasing outward transport by stopping dynein minus end runs. They also found that the transition between the dispersal and aggregation of melanosomes increases dynein-driven motion, decreased myosin V-mediated motion without changing kinesin-driven movement. How these observations might apply to peptidergic vesicle translocation remains unknown.

In the studies presented here, we used two well-known secretagogues; forskolin which stimulates adenylyl cyclase, thus increasing intracellular cAMP levels, and high extracellular $K^{+,}$ which depolarizes the cells and promotes calcium influx, both of which we have shown to stimulate secretion of OFQ peptides from the NS20Y cells. In the case of forskolin, increasing intracellular cAMP levels points to the protein kinase A (PKA) pathway. However, we found inhibitors of PKA (H89) did not inhibit forskolin-stimulated OFQ secretion, while mitogen-activated-protein-kinase (MAPKs) inhibitor PD98059 did inhibit forskolin-stimulated peptide secretion (Allen, unpublished results). The MAPK pathway, possibly interacting with small GTPases regulating motor activity is an intriguing possibility.

We have acquired novel data regarding the regulation of peptidergic vesicle mobility by forskolin stimulation of cAMP production. We found that forskolin stimulation increased vesicle velocities markedly, while depolarization with high K^+ did not; however, both secretagogues increase OFQ peptide secretion. When we analyzed the data for changes in the number of stops a vesicle made in the presence of either forskolin or high K^+, we found no significant difference. This implies that neither secretagogue caused major alterations in the number of interactions a vesicle had with the motor and microtubule, perhaps suggesting that the increase in vesicle mobility by forskolin is due to a 'gas pedal', or some kind of modification of the motor, vesicle, or accessory protein-producing vesicle acceleration that is regulated by cAMP-induced phosphorylation. In addition, the data imply that forskolin treatment induced longer excursions and perhaps longer contact between the motor and the peptidergic vesicles.

The studies presented here are the first to describe secretagogue regulation of peptidergic vesicle mobility. Further studies will focus on other classes of secretagogues and regulation of vesicle mobility, as well as the role of the cytoskeleton in modulating delivery of these chemical messages to their release sites.

Materials and Methods

Construction of expression vectors

The OFQ/eGFP fusion vector was created via overlap-extension PCR. The OFQ coding sequence was PCR-amplified from the mouse OFQ plasmid (33) using the M13 reverse primer (5′-agc gga taa caa ttt cac aca gga) and primer OFQ/eGFP (5′-tg cac cag aat ggt aat gtg/atg gtt cct ggg ggg aa). The OFQ/eGFP primer corresponded to the last 20 bp of the OFQ coding sequence (with no stop codon) and the first 20 bp of the eGFP coding sequence (pEGP-1, Clontech) and provided the overlap between OFQ and eGFP. The resulting fragment was cut with EcoRI and NotI and ligated to EcoRI/NotI cut pcDNA3.0 expression vector (Invitrogen). All vectors and PCR products were verified by sequencing. The JPA5-YFP plasmid was a generous gift of the Gary Banker Laboratory. OFQ was ligated in at the EcoRI and BamHI of the multiple cloning site upstream of the yellow (Y)FP of the YFP-JPA5 plasmid. The soluble CFP was the pECFP-C1 4.7 Kb plasmid from Clontech Laboratories Inc.

Generation of stable NS20Y cells expressing OFQ/eGFP

Mouse neuroblastoma NS20Y cells (20) were grown in DMEM containing 10% FBS and penicillin/streptomycin. Cultures (6-cm dishes) of NS20Y cells were transfected with 10 μg of the OFQ/eGFP plasmid using a calcium phosphate kit from vendor (Invitrogen). After 48 h, cells were washed with DMEM and the medium was replaced with DMEM containing 600 μg of G418. After 3 weeks, with a medium change every 2–3 days, colonies were screened by fluorescence and picked. After transfer to 6-well plates, colonies were rescreened by fluorescence and single-cell clonal populations generated by limiting dilution in 24-well plates. Eight separate lines were generated and the clonal line designated OFQ/eGFP subclone #1 (SC1) was used in the studies described here.

Transfection of primary cultures of hippocampal neurons

Primary cultures of hippocampal neurons were prepared as described (34,35). After 7–9 days, the cultures were transfected with 1–2 μg of the OFQ/eGFP, CFP or OFQ/YFP plasmids using optimized conditions from vendor protocol (LipofectAMINE 2000, Invitrogen). After 48 h, transfected cultures were used for either live-cell imaging or immunostaining of relevant proteins.

Immunofluorescent staining

Hippocampal neurons and NS20Y cells were fixed and permeabilized as previously described (36). The localization of endogenously expressed chromogranin A (ChrA) in NS20Y cells and hippocampal neurons was determined with a ChrA-specific antibody (sc1448) obtained from Santa Cruz Biotechnology (Santa Cruz, CA) and was used at a dilution of 1 : 100. The secondary antiserum (Cy3, donkey anti-goat) was used at a dilution of 1 : 500. MAP2 staining was performed with a primary antisera obtained from Sigma (AP20, 1 : 400) and the secondary antiserum was obtained from Jackson Laboratories (anti-mouse IgG, 1 : 700). Cells were imaged with a Leica DM-IRBE microscope at 63×, using a Princeton Instruments Micromax CCD camera and wide-field epifluorescence. Image analysis was performed using MetamorphÆ Imaging System software (Universal Imaging Corporation) as described below.

Live-cell imaging

Cultures of NS20Y cells were sealed in a heated chamber (Warner Instrument Corporation) and perfused at a rate of approximately 1 ml/min for the first minute (30 frames) with control solution. Then either medium containing 10 μM forskolin or medium containing 60 mM KCl, adjusted for isotonicity, was perfused into the chamber. The control solution was, in mM, glucose 22, $CaCl_2$ 1.26, KH_2PO_4 0.44, $MgCl_2$ 0.49, $MgSO_4$ 0.41, Na_2HPO_4 0.34, HEPES 10, KCl 5.37, NaCl 136. The high K^+ solution was adjusted to 60 mM KCl and the NaCl adjusted to 82.3 mM. A chamber system heater

controller and in-line heater (Warner Instrument Corporation) maintained the perfusion solutions at 37 °C. Hippocampal cultures were perfused for 2.5 min (60 frames) in the control solution. Hippocampal neurons and NS20Y cells were imaged with a Leica DM-IRBE microscope with 63× oil immersion magnification and epifluorescence. Digital images were acquired with a Princeton Instruments Micromax CCD camera, with an exposure time of 600 ms and a total time of 2.6 s in between frames. Vesicle movement was analyzed with MetaMorph® Imaging System (MM®IS) software. We also used the pixel function of MM®IS software to measure the upper limit of peptidergic vesicle size.

Tracking single vesicles and data analysis

Vesicle transport was analyzed using progressive time-lapse digital images, or stacks. Single vesicles were tracked through a stack using the 'track points' function of the Metamorph® Imaging System software. Data generated from a vesicle's movement was included in the analysis only if it could be followed throughout the entire stack (60 frames, approximately 2.5 min) (37). The 'track points' function visually recorded track patterns and generated image measurements, including distance and velocity. The individual statistical analyses used are described in the figure legends.

Acknowledgments

We would like to thank Dr Stefanie Kaech, Manager of the CROET Live Cell Imaging Center. We also thank Barbara Smoody for the hippocampal cultures, Dr Bernard Sampo for incisive discussions, Michael Lasarev for statistical analysis and Harlene Finn for administrative support. This work was supported by National Institutes of Health DA11282 to RGA.

References

1. Bean AJ, Zhang X, Hokfelt T. Peptide secretion: what do we know? FASEB 1994;8: 630–638.
2. Wacker I, Kaether C, Kromer A, Migala A, Almers W, Gerdes HH. Microtubule-dependent transport of secretory vesicles visualized in real time with a GFP-tagged secretory protein. J Cell Sci 1997;110: 1453–1463.
3. Bloom GS, Goldstein LSB. Cruising along microtubule highways: how membranes move through the secretory pathway. J Cell Biol 1998; 140:1277–1280.
4. Sheetz MP. Motor and cargo interactions. Eur J Biochem 1999;262: 19–25.
5. Miyamoto S. Changes in mobility of synaptic vesicles with assembly and disassembly of actin network. Biochim Biophys Acta 1995;1244: 85–91.
6. Doussau F, Augustine GJ. The actin cytoskeleton and neurotransmitter release: an overview. Biochimie 2000;82: 353–363.
7. Dermitzaki E, Gravanis A, Venihaki M, Stournaras C, Margioris AN. Opioids suppress basal and nicotine-induced catecholamine secretion via a stabilizing effect on actin filaments. Endocrinology 2001;142: 2022–2031.
8. Klopfenstein DR, Vale RD, Rogers SL. Motor protein receptors: moonlighting on other jobs. Cell 2000;103: 537–540.
9. Miki H, Setou M, Kaneshiro K, Hirokawa N. All kinesin superfamily protein, KIF, genes in mouse and human. PNAS 2001;98: 7004–7011.
10. Reese EL, Haimo LT. Dynein, dynactin, and kinesin II's interaction with microtubules is regulated during bidirectional organelle transport. J Cell Biol 2000;151: 155–166.
11. De Vos K, Severin F, Van Herreweghe F, Vancompernolle K, Goossens V, Hyman A, Grooten J. Tumor necrosis factor induces hyperphosphorylation of kinesin light chain and inhibits kinesin-mediated transport of mitochondria. J Cell Biol 2000;149: 1207–1214.
12. Okada Y, Sato-Yoshitake R, Hirokawa N. The activation of protein kinase A pathway selectively inhibits anterograde axonal transport of vesicles but not mitochondria transport or retrograde transport*in vivo*. J Neurosci 1995;15: 3053–3064.
13. Burke NV, Han W, Li D, Takimoto K, Watkins SC, Levitan ES. Neuronal peptide release is limited by secretory granule mobility. Neuron 1997;19: 1095–1102.
14. Chao DS, Hay JC, Winnick S, Prekeris R, Klumperman J, Scheller RH. SNARE membrane trafficking dynamics*in vivo*. J Cell Biol 1999;144: 869–881.
15. KaetherC, Salm T, Glombik M, Almers W, Gerdes HH. Targeting of **Q23** green fluorescent protein to neuroendocrine secretory granules: a new tool for real time studies of regulated protein secretion. Eur J Cell Biol 1997;74: 133–142.
16. Sirianni MJ, Fujimoto KI, Nelson CS, Pellegrino MJ, Allen RG. Cyclic AMP analogs induce synthesis, processing, and secretion of prepro nociceptin/orphanin FQ-derived peptides by NS20Y neuroblastoma cells. DNA Cell Biol 1999;18: 51–58.
17. Dotti CG, Sullivan CA, Banker GA. The establishment of polarity by hippocampal neurons in culture. J Neurosci 1988;8: 1454–1468.
18. Han W, Ng Y-K, Axelrod D, Levitan ES. Neuropeptide release by efficient recruitment of diffusing cytoplasmic secretory vesicles. PNAS 1999;96: 14577–14582.
19. Lochner JE, Kingma M, Kuhn S, Meliza CD, Cutler B, Scalettar BA. Real-time imaging of the axonal transport of granules containing a tissue plasminogen activator/green fluorescent protein hybrid. Mol Biol Cell 1998;9: 2463–2476.
20. Hirschberg K, Miller CM, Ellenberg J, Presley JF, Siggia ED, Phair RD, Lippincott-Schwartz J. Kinetic analysis of secretory protein traffic and characterization of golgi to plasma membrane transport intermediates in living cells. J Cell Biol 1998;: 6. **Q24**
21. Nakata T, Terada S, Hirokawa N. Visualization of the dynamics of synaptic vesicle and plasma membrane proteins in living axons. J Cell Biol 1998;140: 659–674.
22. Chuang JZ, Milner TA, Zhu M, Sung CH. A 29 kDa intracellular chloride channel p64H1 is associated with large dense-core vesicles in rat hippocampal neurons. J Neurosci 1999;19: 2919–2928.
23. Ludwig M, Sabatier N, Bull PM, Landgraf R, Dayanithi G, Leng G. Intracellular calcium stores regulate activity-dependent neuropeptide release from dendrites. Nature 2002;418: 85–89.
24. Thorn KS, Ubersax JA, Vale RD. Engineering the processive run length of the kinesin motor. J Cell Biol 2000;151: 1093–1100.
25. Lindesmith L, McIlvain JM Jr, Argon Y, Sheetz MP. Phosphotransferases associated with the regulation of kinesin motor activity. J Biol Chem 1997;272: 22929–22933.
26. Sato-Yoshitake R, Yorifuji H, Inagaki M, Hirokawa N. The phosphorylation of kinesin regulates its binding to synaptic vesicles. J Biol Chem 1992;267: 23930–23936.
27. Lee KD, Hollenbeck PJ. Phosphorylation of kinesin*in vivo* correlates with organelle association and neurite outgrowth. J Biol Chem 1995;270: 5600–5605.
28. Marlowe KJ, Farshori P, Torgerson RR, Anderson KL, Miller LJ, McNiven MA. Changes in kinesin distribution and phosphorylation occur during regulated secretion in pancreatic acinar cells. Eur J Cell Biol 1998;75: 140–152.
29. Lin SX, Ferro KL, Collins CA. Cytoplasmic dynein undergoes intracellular redistribution concomitant with phosphorylation of the heavy chain in response to serum starvation and okadaic acid. J Cell Biol 1994;127: 1009–1019.
30. Niclas J, Allan VJ, Vale RD. Cell cycle regulation of dynein association with membranes modulates microtubule-based organelle transport. J Cell Biol 1996;133: 585–593.

31. Duke T. Push or pull? Teams of motor proteins have it both ways. Proc Natl Acad Sci USA 2002;99: 6521–6523.
32. Gross SP, Tuma MC, Deacon SW, Serpinskaya AS, Reilein AR, Gelfand VI. Interactions and regulation of molecular motors in*Xenopus melanophores*. J Cell Biol 2002;156: 855–865.
33. Quigley DI, McDougall J, Darland T, Zhang GE, Ronnekliev O, Grandy DK, Allen RG. Orphanin FQ is the major OFQ1–17-containing peptide produced in the rodent and monkey hypothalamus. Peptides 1998;19: 133–139.
34. Jareb M, Banker G. Inhibition of axonal growth by brefeldin A in hippocampal neurons in culture. J Neurosci 1997;17: 8955–8963.
35. Burack MA, Silverman MA, Banker G. The role of selective transport in neuronal protein sorting. Neuron 2000;26: 465–472.
36. Withers GS, Higgins D, Charette M, Banker G. Bone morphogenetic protein-7 enhances dendritic growth and receptivity to innervation in cultured hippocampal neurons. Eur J Neurosci 2000;12: 106–116.
37. Pinheiro J, Bates D. Mixed-Effects Models in S and S-PLUS. New York: Springer;2000.

Journal: Traffic
Article: TRA2o022

AUTHOR QUERY FORM

Dear Author,

Queries from the Production Editor are listed on the last page of the proof. The text to which the queries refer is indicated on the proof by numbers (e.g. Q1) in the margin.
Many thanks for your assistance.

Q1 Au: Please provide a short running head

Remarks:

Q2 Au: neuropeptide containing secretory vesicles: OK? or**neuropeptide-containing secretory granules**?

Remarks:

Q3 Au: Please supply keywords

Remarks:

Q4 Au: Neuropeptide containing secretory granules: OK? or**Neuropeptide-containing secretory granules**?

Remarks:

Q5 Au: OK now?

Remarks:

Q6 Please note that the references have been reordered from number**15** onwards (15–18 reordered)

Remarks:

Q7 Au: the number of stops a vesicle made was only about 4–5 during: OK now?

Remarks:

Q8 Au: ChA or**ChrA**?

Remarks:

Q9 Au: at the site denoted in the Footnotes (Traffic.com): Please check

Remarks:

Q10 Au: Burke et al. (13): OK now? Or is it important to include the year?

Remarks:

Q11 Au: Han et al. (18): OK now?

Remarks:

Q12 Au: Is**partical** spelt correctly? Or**particle**? or**partial**?

Remarks:

Q13 Au: please check reference numbers. They should appear (journal format) but you may add dates if these are important

Remarks:

Q14 Au: Is the text OK: **by stopping dynein minus end runs**

Remarks:

Q15 Au: increase: OK? or**increased**?

Remarks:

Q16 Au: Please supply more details of**Clontech**

Remarks:

Q17 Au: Please supply more details of**Invitrogen**

Remarks:

Q18 Au: chromogranin: spelling OK now? (you had**chromagranin)**. Please check spelling in Figure 1)

Remarks:

Q19 Au: Please supply more details of**Sigma**

Remarks:

Q20 Au: Please supply more details of**Jackson Laboratories**

Remarks:

Q21 Au: Please supply more details of**Warner Instrument Corporation**

Remarks:

Q22 Au: KH_2PO_4: OK now?

Remarks:

Q23 Au: This was ref. 18: please check refs 15–18.

Remarks:

Q24 Au: Please supply missing volume number

Remarks:

Q25 Au: chromogranin: spelling? see Figure 1 and main text (**chromagranin**)

Remarks:

Q26 Au: Figure 4: please correct this in the proof (this is Fig. 4)

Remarks:

Q27 Au: The graphs show the rates of vesicles in individual frames: OK now?

Remarks: